Molecular Crystals and Liquid Crystals
Publication details, including instructions for authors and subscription information:
http://www.tandfonline.com/loi/gmcl20

# Doping Effect of Silole Derivative in Coumarin 30 Photoconductive Film

Toshikatsu Sakai [a], Hokuto Seo [a], Satoshi Aihara [a], Misao Kubota [a], Norifumi Egami [a], Keita Mori [b], Takeshi Fukuda [b], Ken Hatano [b] & Norihiko Kamata [b]

[a] NHK Science & Technology Research Laboratories, Tokyo, Japan
[b] Department of Functional Materials Science, Graduate School of Science and Engineering, Saitama University, Saitama, Japan

Version of record first published: 27 Sep 2012.

To cite this article: Toshikatsu Sakai , Hokuto Seo , Satoshi Aihara , Misao Kubota , Norifumi Egami , Keita Mori , Takeshi Fukuda , Ken Hatano & Norihiko Kamata (2012): Doping Effect of Silole Derivative in Coumarin 30 Photoconductive Film, Molecular Crystals and Liquid Crystals, 568:1, 74-81

To link to this article: http://dx.doi.org/10.1080/15421406.2012.710188

*Mol. Cryst. Liq. Cryst.*, Vol. 568: pp. 74–81, 2012

ISSN: 1542-1406 print/1563-5287 online
DOI: 10.1080/15421406.2012.710188

Taylor & Francis
Taylor & Francis Group

# Doping Effect of Silole Derivative in Coumarin 30 Photoconductive Film

TOSHIKATSU SAKAI,[1,*] HOKUTO SEO,[1] SATOSHI AIHARA,[1] MISAO KUBOTA,[1] NORIFUMI EGAMI,[1] KEITA MORI,[2] TAKESHI FUKUDA,[2] KEN HATANO,[2] AND NORIHIKO KAMATA[2]

[1]NHK Science & Technology Research Laboratories, Tokyo, Japan
[2]Department of Functional Materials Science, Graduate School of Science and Engineering, Saitama University, Saitama, Japan

*To obtain a highly sensitive and color selective photodetector for an image sensor, silole-derivative-doped coumarin 30 photoconductive films were fabricated. The silole-doped films showed excellent color selectivites only in the blue region of visible light. The dark current in the films decreased when the silole-doping concentration was increased, which reached down to 1.0 × $10^{-9}$ A/cm$^2$ at −10 V in the 80%-silole-doped film. The 50%-silole-doped device showed high external quantum efficiency up to 60% along with the excellent color selectivity.*

**Keywords** coumarin 30; image sensor; organic photoconductor; silole; co-evaporation



## Introduction

Organic semiconductor materials have been extensively studied with regard to their potential optical applications to light-emitting diodes [1], thin-film transistors (TFTs) [2], and photovoltaic devices [3,4]. Photoconduction in organic materials is of particular interest for its potential photo-detective application [5–9]. Meanwhile, we have been developing a new type of image sensor that is overlaid with three different organic photoconductive layers [10–13]. We take advantage of the color selectivity of organic materials and arrange for each layer to be sensitive to only one of the primary colors. This type of sensor has huge potential for use in high-resolution compact color cameras, especially compared with conventional sensors. Conventional sensors, such as charge-coupled devices (CCDs) and complementary metal-oxide semiconductor (CMOS) devices, require a color filter array or a dichroic prism to obtain color pictures. The color filter array deteriorates image resolution due to its spatial color separation structure with planar mosaic array, and also, it is difficult to reduce the size of the dichroic prism and related optical system.

In previous studies, we have shown that organic photoconductive films have suitable characteristics for the photoelectric conversion part of a stacked image sensor, including excellent color selectivity [10,14] and high resolution (as revealed by using them in camera

*Address corresponding to Toshikatsu Sakai, NHK Science & Technology Research Laboratories, 1-10-11 Kinuta, Setagaya-ku, Tokyo 157-8510, Japan.Tel: +81-3-5494-3215 Fax: +81-3-5494-3278. E-mail: sakai.t-ka@nhk.or.jp

tubes) for high-definition television [15,16]. We have also fabricated a stack-type color image sensor with blue-, green-, and red-sensitive organic photoconductive films, each of which has a signal readout circuit with an oxide semiconductor TFT array, and obtained color images from the fabricated sensors [12,13].

In order to improve the performance of the stack-type image sensor, enhancing the quantum efficiencies and color selectivities of the organic photoconductive films is quite important. In our previous study, we fabricated two types of blue-sensitive organic photoconductive film consisting of coumarin 30 with and without fullerene ($C_{60}$) doping, and we evaluated the effects of $C_{60}$ doping as an electron acceptor on the photoconductive properties of the films [17]. The external quantum efficiency (EQE) was increased by $C_{60}$ doping and reached 64% at the relatively low bias voltage of 10 V. However, $C_{60}$-doped coumarin 30 film has a weak absorption in the wavelength range from 500 to 700 nm due to the photoabsorption of $C_{60}$. This absorption causes a photocurrent in the green and red light regions that degrades the color selectivity of a blue-sensitive photodetector. There have been studies on the effects of doping various silole-derivatives in photoconductive polymers by spin coating [18,19]. Silole derivatives are suitable dopants for blue-sensitive photodetectors because they have a wide bandgap of more than 2.4 eV, which can transmit green and red light.

In this study, we investigated the effect of doping 1,1-dimethyl-2,5-bis(*N,N*-dimethylaminophenyl)-3,4-diphenylsilole ($NMe_2$-silole) in coumarin 30 photoconductive films for use in a blue-sensitive photodetector with a good color selectivity and a high EQE. We fabricated sandwich cells of the photoconductive films with various doping concentrations, and then evaluated their photoconductive properties with optical and electrical measurements.



## Experimental

Figure 1 illustrates cross-sectional view of the sandwich cells with the molecular structures of the organic materials used in this study. The fabrication process of the device was as follows. Firstly, 80-nm-thick photoconductive layers consisting of $NMe_2$-silole doped coumarin 30 were deposited on indium-tin-oxide (ITO)-coated glass substrates by co-evaporation using a separate source. The doping ratio of $NMe_2$-silole to coumarin 30 was 20, 50, and 80% in volume percentage. Next, 20-nm-thick tris(8-hydroxyquinolinato)aluminium ($Alq_3$) buffer layers and 30-nm-thick aluminum electrodes were evaporated on the photoconductive layers. Reference devices consisting of ITO/coumarin 30/$Alq_3$/Al and ITO/ $NMe_2$-silole/$Alq_3$/Al were also fabricated. All the evaporation processes were continuously performed in a vacuum chamber under a pressure of $10^{-5}$ Pa. The active area of these devices was $2.0 \times 3.0$ mm$^2$. Current-voltage characteristics and photoresponse characteristics of the devices were measured with a spectral response measurement system (YQ-250, Bunkokeiki Co. Ltd.).

## Results and Discussion

### *Photoconductive Properties*

The current-voltage characteristics of neat coumarin 30 and the 50% silole-doped device with and without monochromatic light irradiation, whose wavelength and incident power were 420 nm and 50 $\mu$W/cm$^2$, respectively, are shown in Fig. 2. When the ITO electrode

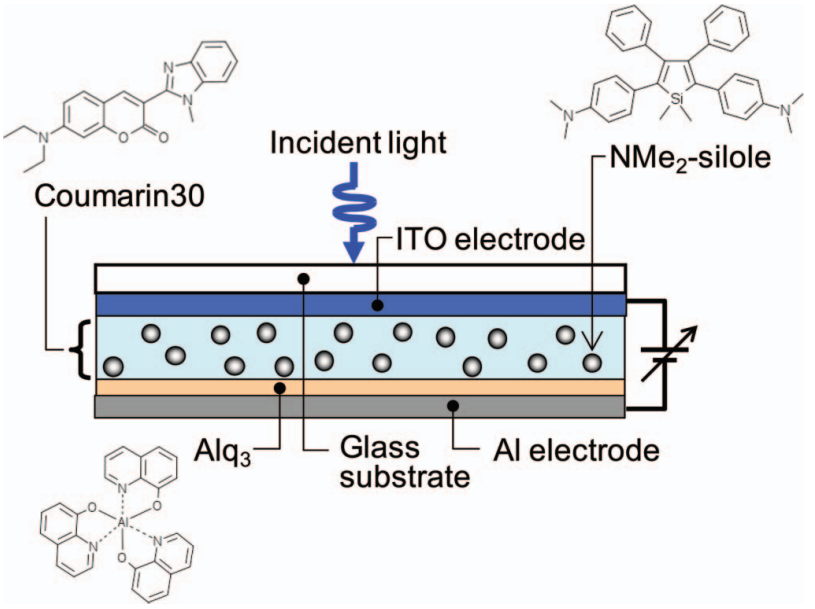


**Figure 1.** Cross-sectional view of fabricated device with molecular structures in this study.



was positively biased ($V_{ITO+}$), the dark current in the coumarin 30 device fluctuated at around $10^{-9}$ A/cm$^2$, while that in 50% silole-doped device rapidly increased as the applied voltage was increased. In contrast, when the ITO electrode was negatively biased ($V_{ITO-}$), the dark current was drastically suppressed in the 50% silole-doped device, although it increased as the applied voltage was increased in the coumarin 30 device. The dark current in the 50% silole-doped device was as small as $2.3 \times 10^{-9}$ A/cm$^2$ at $-5$ V and $3.9 \times 10^{-9}$ A/cm$^2$ at $-10$ V. It is considered that this change of the dark current characteristics

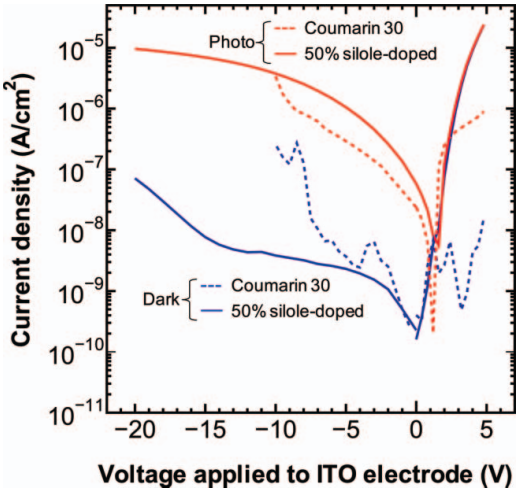


**Figure 2.** Current-voltage characteristics of neat coumarin 30 and 50% silole-doped devices.

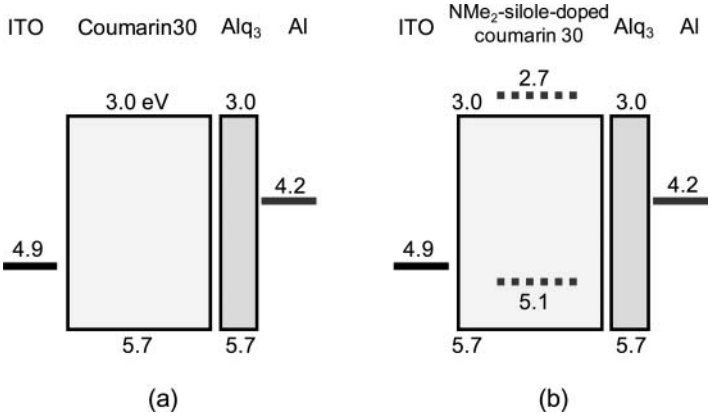


**Figure 3.** Energy diagrams of fabricated devices, (a) coumarin 30 device, (b) silole-doped device.

by silole-doping originates from the energy level difference between the ITO electrode and the photoconductive layers. The energy level diagrams of both devices are shown in Fig. 3. The ionization potentials of coumarin 30 and $NMe_2$-silole are 5.7 and 5.1 eV, respectively. When $V_{ITO+}$ was applied, hole injection was blocked due to the potential barrier at the ITO/coumarin 30 interface in the coumarin 30 device (Fig. 3(a)). On the other hand, the potential barrier at the ITO/silole-doped layer in the silole-doped device was reduced because of the higher ionization potential of $NMe_2$-silole (5.1 eV) in the layer (Fig. 3(b)), resulting in the rapid increase in dark current as $V_{ITO+}$ increased (Fig. 2). When $V_{ITO-}$ was applied, in contrast, the electron injection from the ITO to the silole-doped layer was inhibited owing to the higher electron affinity (2.7 eV) of $NMe_2$-silole than that of coumarin 30 (3.0 eV), and this energy level difference induced the reduction of the dark current by silole doping.

The photocurrent in the silole-doped device at $V_{ITO-}$ was larger than that of the coumarin 30 device at the same voltage. On the other hand, there was no difference between the photocurrent and the dark current in the silole-doped device at $V_{ITO+}$, which indicates that the injection current from the electrode to the photoconductive layer was dominant at $V_{ITO+}$.

Figure 4 shows the current-voltage characteristics of the silole-doped devices with various doping concentrations with and without monochromatic light irradiation (420 nm, 50 $\mu W/cm^2$). The dark current decreased as the doping concentration was increased, which reached down to $1.0 \times 10^{-9}$ A/cm$^2$ at $-10$ V in the 80%-doped device. However, the 80%-doped device also reduced the photocurrent relative to those of 20 and 50%-doped devices. These results suggest that excess doping of silole induces a decreasing of the photocurrent.

Considering these photocurrent and dark current characteristics, 50% is the optimum value of silole-doping concentration.

### *Spectral Photoresponse Characteristics*

The spectral photoresponse characteristics of the 50% silole-doped device are shown in Fig. 5. As shown in the figure, the device had a sensitivity only to the blue region in the visible range at all applied voltages. The 20, 50, and 80% silole-doped devices also showed a similar spectral shape. The EQE, defined as the number of output electrons divided by

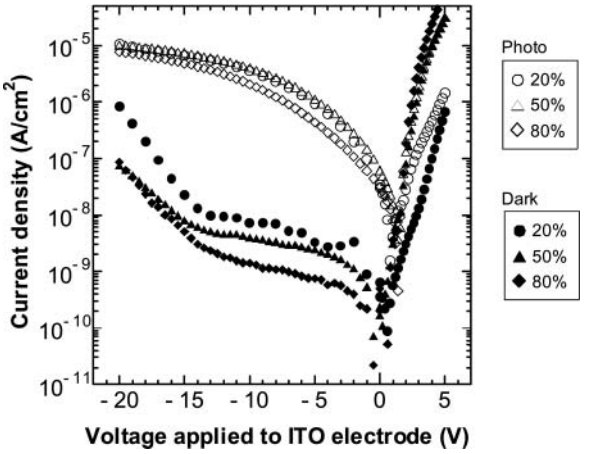


**Figure 4.** Current-voltage characteristics of silole-doped devices with various concentrations of silole.

the number of irradiated photons, increased as the absolute value of the voltage applied to the ITO electrode was increased, and it reached almost 60% at −20 V.

The influence of the silole-doping concentration on the EQE at the voltage of −10 V is shown in the inset of Fig. 5. Compared to neat coumarin 30 device (0% of the horizontal axis in the inset of Fig. 5), EQEs of silole-doped devices increased with increasing silole concentration from 20 to 50%. However, the EQE of the 80%-silole-doped device became lower than that of the neat coumarin 30 device. It also indicates that 50% is the optimum value of silole-doping concentration from the viewpoint of quantum efficiency.

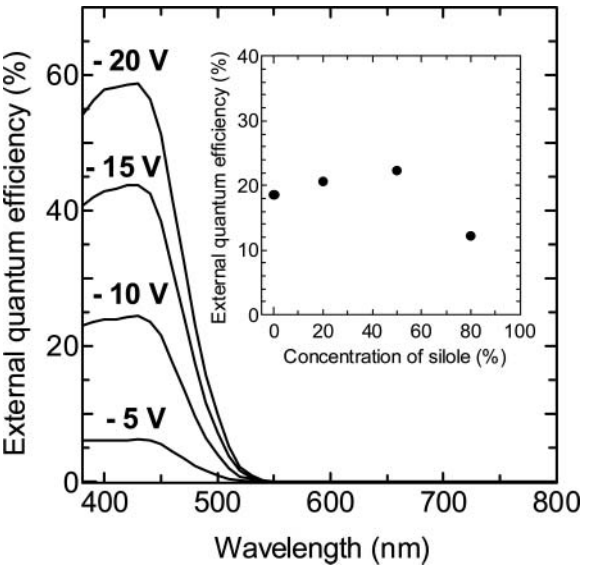


**Figure 5.** Spectral photoresponse characteristics of 50% silole-doped device. Bias voltage was applied from −5 to −20 V. Inset represents Silole-doping concentration influence on external quantum efficiencies.

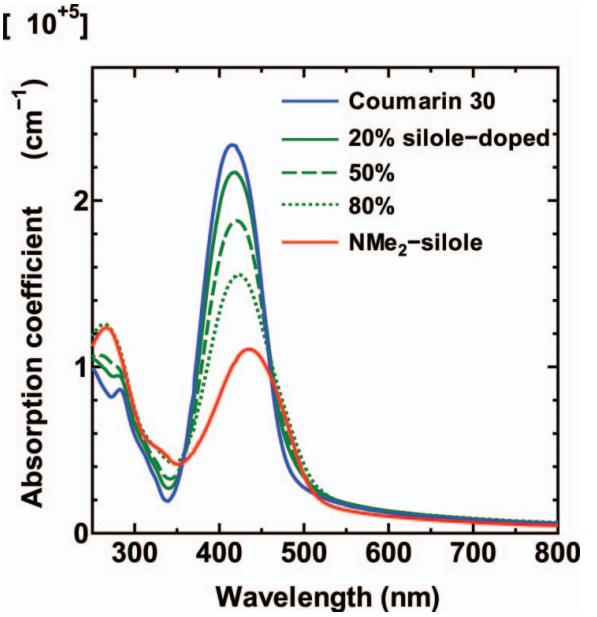


**Figure 6.** Absorption spectra of fabricated films and neat $NMe_2$-silole film.

Here we discuss the doping effect of $NMe_2$-silole on the EQE of these films. Figure 6 shows absorption spectra of the fabricated films with that of neat $NMe_2$-silole film. The absorption coefficient decreased with increasing silole-doping ratio. However, the EQE increased with increasing the ratio up to 50%. It is speculated that this EQE enhancement was caused by the increase of the charge dissociation at the interface between coumarin 30 and $NMe_2$-silole molecules, which is similar to the charge dissociation mechanism in bulk heterojunction organic solar cells [20]. In this case, coumarin 30 acted as an electron acceptor, while $NMe_2$-silole acted as an electron donor, considering from the difference of electron affinities and ionization potentials between coumarin 30 and $NMe_2$-silole shown in Fig. 3(b).

On the other hand, it is considered that the decrease of the photoabsorption in the photoconductive layer due to the low absorption coefficient of $NMe_2$-silole became dominant at the silole-doping concentration of 80%, and the decrease of the EQE occurred.

We previously reported on the enhancement of EQE caused by doping $C_{60}$ into coumarin 30 film ($C_{60}$-doped device) [17]. Figure 7 shows the spectral photoresponse of the silole-doped device in comparison to the $C_{60}$-doped device. The EQE of the $C_{60}$-doped device reached 64% at an applied voltage of 10 V, but the small photocurrent in the green to red light region which originated from the absorption of $C_{60}$ molecules degraded the wavelength selectivity. By substituting $NMe_2$-silole for $C_{60}$, excellent wavelength selectivity in the blue light region was able to be obtained as shown in Fig. 7. The operation voltage of the silole-doped device ($-20$ V at 60% quantum efficiency), however, needs to be lowered as well as that of the $C_{60}$-doped device ($-10$ V at 64%). These results demonstrate that doping silole derivative in coumarin 30 is an effective means of improving the EQE without degrading the wavelength selectivity in blue-sensitive films. As our next step, we will search for other silole derivatives to lower the operating bias voltage.

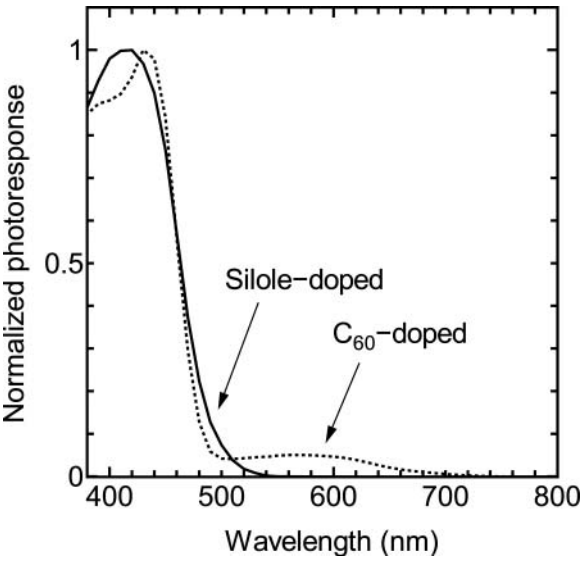


**Figure 7.** Spectral photoresponse of silole-doped device and $C_{60}$-doped device.

## Conclusion

$NMe_2$-silole-doped coumarin 30 photoconductive films with various doping concentrations were fabricated and their photoconductive properties were measured. The dark current of the films decreased when the silole-doping concentration was increased, which reached down to $1.0 \times 10^{-9}$ A/cm$^2$ at $-10$ V in the 80%-doped device. The mechanism of that reduction of the dark current by silole-doping was attributed to the energy level difference between coumarin 30 and $NMe_2$-silole. The 50%-silole-doped device had a high EQE of 60% along with excellent color selectivities only in the blue light region. Experiment results revealed that 50% is the optimum value of silole-doping concentration for coumarin 30 film, thus demonstrating that silole-doped coumarin 30 film is an attractive candidate for blue-sensitive photoconductive film in stack-type color image sensors.

## References

[1] Tang, C. W., & VanSlyke, S. A. (1987). *Appl. Phys. Lett.*, *51*, 913.
[2] Lin, Y. Y., Gundlach, C. J., Nelson, S. F., & Jackson, T. N. (1997). *IEEE Electron Device Lett.*, *18*, 606.
[3] Tang, C. W. (1986). *Appl. Phys. Lett.*, *48*, 183.
[4] Oregan, B., & Gratzel, M. (1991). *Nature*, *353*, 737.
[5] Zukawa, T., Naka, S., Okada, H., & Onnagawa, H. (2002). *J. Appl. Phys.*, *91*, 1171.
[6] Kudo, K., & Moriizumi, T. (1981). *Appl. Phys. Lett.*, *39*, 609.
[7] Street, R. A., Mulato, M., Lau, R., Ho, J., Graham, J., Popovic, Z., & Hor, J. (2001). *Appl. Phys. Lett.*, *78*, 4193.
[8] Nausieda, I., Ryu, K., Kymissis, I., Akinwande, A. I., Bulovic, V., & Sodini, C. G. (2008). *IEEE Trans. Electron Devices*, *55*, 527.
[9] Hiramoto, M., Imahigashi, T., & Yokoyama, M. (1994). *Appl. Phys. Lett.*, *64*, 187.
[10] Aihara, S., Hirano, Y., Tajima, T., Tanioka, K., Abe, M., Saito, N., Kamata, N., & Terunuma, D. (2003). *Appl. Phys. Lett.*, *82*, 511.

[11] Seo, H., Aihara, S., Watabe, T., Ohtake, H., Kubota, M., & Egami, N. (2007). *Jpn. J. Appl. Phys.*, *46*, L1240.
[12] Aihara, S., Seo, H., Namba, M., Watabe, T., Ohtake, H., Kubota, M., Egami, N., Hiramatsu, T., Matsuda, T., Furuta, M., Nitta, H., & Hirao, T. (2009). *IEEE Trans. Electron Devices*, *56*, 2570.
[13] Seo, H., Aihara, S., Watabe, T., Ohtake, H., Sakai, T., Kubota, M., Egami, N., Hiramatsu, T., Matsuda, T., Furuta, M., & Hirao, T. (2011). *Jpn. J. Appl. Phys.*, *50*, 024103.
[14] Fukuda, T., Komoriya, M., Kobayashi, R., Ishimaru, Y., & Kamata, N. (2009). *Jpn. J. Appl. Phys.*, *48*, 04C162.
[15] Aihara, S., Miyakawa, K., Ohkawa, Y., Matsubara, T., Takahata, T., Suzuki, S., Egami, N., Saito, N., Tanioka, K., Kamata, N., & Terunuma, D. (2003). *Jpn. J. Appl. Phys. 42*, L801.
[16] Aihara, S., Miyakawa, K., Ohkawa, Y., Matsubara, T., Takahat,a T., Suzuki, S., Kubota, M., Tanioka, K., Kamata, N., & Terunuma, D. (2005). *Jpn. J. Appl. Phys.*, *44*, 3743.
[17] Seo, H., Aihara, S., Kubota, M., & Egami, N. (2010). *Jpn. J. Appl. Phys.*, *49*, 111601.
[18] Fukuda, T., Kobayashi, R., Kamata, N., Aihara, S., Seo, H., Hatano, K., & Terunuma, D. (2010). *Jpn. J. Appl. Phys.*, *49*, 01AC05.
[19] Kobayashi, R., Fukuda, T., Suzuki, Y., Hatano, K., Kamata, N., Aihara, S., Seo, H., & Terunuma, D. (2010). *Mol. Cry. Liq. Cry.*, *519*, 206.
[20] Gunes, S., Neugebauer, H., & Sariciftci, N. S. (2007). *Chem. Rev.*, *107*, 1324.